International Journal of Automotive Technology, Vol. 7, No. 5, pp. 571–577 (2006)

1229-9138/2006/029-07

EVALUATION OF DYNAMIC TENSILE CHARACTERISTICS OF POLYPROPYLENE WITH TEMPERATURE VARIATION

J. S. KIM[1], H. HUH[1]*, K. W. LEE[2], D. Y. HA[2], T. J. YEO[2] and S. J. PARK[2]

[1]Department of Mechanical Engineering, Korea Advanced Institute of Science and Technology, Daejeon 305-701, Korea
[2]Hyundai MOBIS Technical Research Center, 80-10 Mabuk-dong, Guseong-gu, Yongin-si, Gyeonggi 449-912, Korea

(Received 25 October 2005; Revised 9 November 2005)

ABSTRACT–This paper deals with dynamic tensile characteristics for the polypropylene used in an IP (Instrument Panel). The polypropylene is adopted in the dash board of a car, especially PAB (Passenger Air Bag) module. Its dynamic tensile characteristics are important because the PAB module undergoes high speed deformation during the airbag expansion. Since the operating temperature of a car varies from –40°C to 90°C according to the specification, the dynamic tensile tests are performed at a low temperature (–30°C), the room temperature (21°C) and a high temperature (85°C). The tensile tests are carried out at strain rates of six intervals ranged from 0.001/sec to 100/sec in order to obtain the strain rate sensitivity. The flow stress decreases at the high temperature while the strain rate sensitivity increases. Tensile tests of polymers are rather tricky since polymer does not elongate uniformly right after the onset of yielding unlike the conventional steel. A new method is suggested to obtain the stress–strain curve accurately. A true stress–strain curve was estimated from modification of the nominal stress–strain curves obtained from the experiment. The modification was carried out with the help of an optimization scheme accompanied with finite element analysis of the tensile test with a special specimen. The optimization method provided excellent true stress–strain curves by enforcing the load response coincident with the experimental result. The material properties obtained from this paper will be useful to simulate the airbag expansion at the normal and harsh operating conditions.

KEY WORDS : Dynamic tensile test, Thermoplastics, Polypropylene, Temperature, True stress, True strain

1. INTRODUCTION

Polymers are continuously applied with increased frequency to auto-body applications subjected to high strain rate and harsh climate. Since the mechanical behavior of thermoplastics is important to design and analyze the engineering problems, it has been of a great interest to many researchers. The mechanical behavior with the variation of temperature is of great importance because the operating temperature of a car is known to vary from –30°C to 110°C according to the handbook (The Korean Society of Automotive Engineers, 1996). The dynamic material properties are necessary to estimate the high speed deformation. The effect of the strain rate and temperature on the strain hardening response of polymers has been widely studied in previous investigations. Machida and Lee (1988) studied the deep drawing of polypropylene sheets with various temperatures. The deformation behavior of various polymers was studied over a range of strain rates by Walley *et al.* (1989). Among their conclusions some materials such as polyvinylidene difluoride show no strain hardening but rather strain softening at high strain rates because of adiabatic heating effect concomitant with the high strain rate tests. The flow stress decreases remarkably by elevating the temperature and increases as the strain rate increases (Arruda *et al.*, 1995). The effects of the temperature, the strain rate and the composition on the epoxy thermosets were also studied (Cook *et al.*, 1998; Mayr *et al.*, 1998). The effects of the temperature and the stem length on the yield stress were evaluated at a strain rate of 10^{-2}/sec, over a temperature range from –60°C to 60°C (Brooks and Mukhtar, 2000). Kim (2006) also investigated the strain rate sensitivity of a polypropylene as a core material used in the sandwich sheet. It is clearly verified that the thermoplastics are effected by both the temperature and the strain rate.

Since thermoplastics deforms inhomogeneously right after the onset of yielding unlike common steels, the conventional extensometry methods to obtain a true stress–strain curve are not available any longer. There are

*Corresponding author. e-mail: hhuh@kaist.ac.kr

two ways to deal with this problem: the first way is to select a test specimen that deforms uniformly; the second way is to derive a good estimation by thorough observation of the deformation patterns. Necking propagation for round and flat specimens were observed at the room temperature and at several strain rates (Marquez-Lucero *et al.*, 1989). The evolution of the volumetric strain was determined and applied to stress–strain behavior by using a novel video-controlled testing system (G'Sell *et al.*, 2002). Recently, a new method for simultaneously measuring strains in all three dimensions during a uniaxial tension test was introduced to obtain a true stress–strain curve and volumetric strain in neat and rigid-filled polymers (Parsons *et al.*, 2005). Kang and Huh (2000) and Huh *et al.* (2003) adopted Johnson–Cook constitutive model in order to apply the dynamic material properties of steel sheets to crash analysis of an auto-body.

In this paper, a new method to obtain true stress–strain curves is proposed using the finite element analysis and an optimization scheme. First, finite element analysis of tensile tests with the new specimen is performed by using the previous experimental results from the conventional extensometry method. Another finite element analysis is, then, carried out by using optimized true stress–strain curves in order to confirm the validity and accuracy of the stress–strain curves modified. The stress–strain curves are indispensable for information about tensile characteristics of the polypropylene used in an instrument panel of a vehicle at various temperatures and strain rates. The effect of heat aging is also discussed by comparing it with the experimental results without heat aging. Consquently, modification of stress–strain curves using the finite element method is suggested on the basis of experimental results.

2. EXPERIMENT

2.1. Specimen Preparation

As a specimen for uniaxial tensile tests, the ASTM IV standard specimen was chosen as shown in Figure 1. The gauge length is 33 mm, the width is 6 mm, and the thickness is 2 mm. Since the polymer specimen undergoes localized deformation after the onset of yielding and produces inaccurate stress–strain curves in the tensile test, the stress–strain curves obtained with the specimen needs to be modified for an accurate true stress–strain relation. In order to modify the stress–strain curve obtained from experiments, a new specimen was prepared for experiments and finite element analysis as shown in Figure 2.

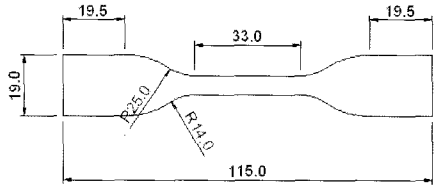

Figure 1. ASTM IV standard specimen.

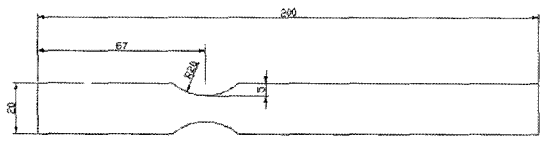

Figure 2. New specimen.

2.2. Experimental Apparatus

The quasi-static tensile test was performed at the strain rate of 0.001/sec with Inston 5583 in an environmental chamber for low and high temperature tests. The dynamic tensile test corresponding to strain rates ranged from 1/sec to 100/sec were carried out in an environmental chamber with a High Speed Material Testing Machine (Lim *et al.*, 2005).

2.3. Experimental Results

Tensile tests were performed under the three different

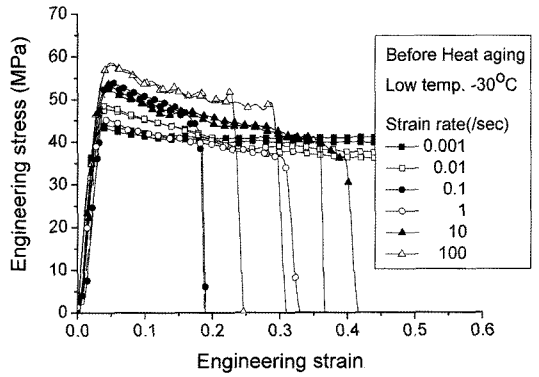

Figure 3. Engineering stress–strain curves at the low temperature (–30°C) for a polypropylene.

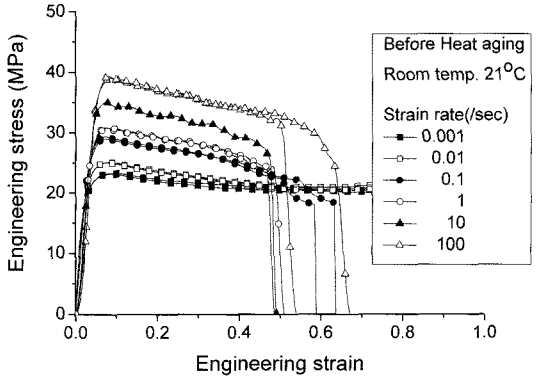

Figure 4. Engineering stress–strain curves at the room temperature (21°C) for a polypropylene.

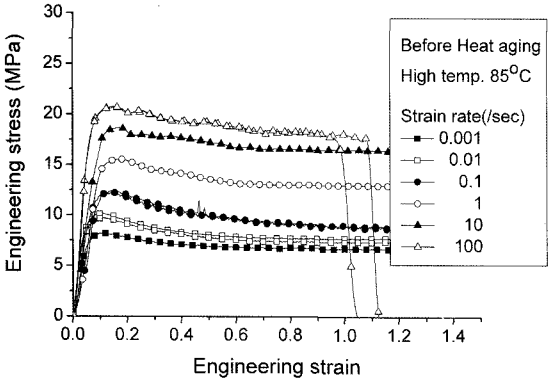

Figure 5. Engineering stress–strain curves at the high temperature (85°C) for a polypropylene.

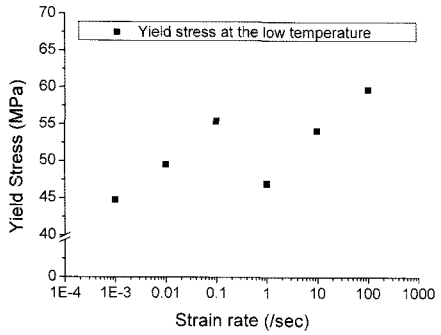

Figure 6. Strain rate sensitivity of a polypropylene at the low temperature (−30°C).

temperature conditions: a low temperature of −30°C; the room temperature of 21°C; and a high temperature of 85°C. The tests were carried out at six strain rates of 0.001, 0.01, 0.1, 1, 10 and 100/sec before and after the specimen was heat-aged. Figure 3 shows engineering stress–strain curves obtained at the low temperature. Engineering stress–strain curves at the room and high temperature are also shown in Figure 4 and 5 respectively. The flow stress at the low temperature has fluctuation with respect to the strain rate while the flow stress at the room and high temperature increases as the strain rate increases. Figure 3 shows that the flow stress at the strain rate of 0.1/sec is higher than that at the strain rate of 1/sec as well as the yield stress. The variation of the yield stress is demonstrated in Figure 6 with respect to the strain rate at the low temperature. As shown in Figure 7, the yield stress at the strain rate of 100/sec is about 30% higher than that of 0.001/sec at the low temperature, 70% higher at the room temperature and 150% higher at the high temperature. This results show that the strain rate sensitivity increases as the temperature increases. Figure 7 also demonstrates the variation of the flow stress with respect to the temperature. The yield stress at the strain rate of 0.001/sec at the low temperature

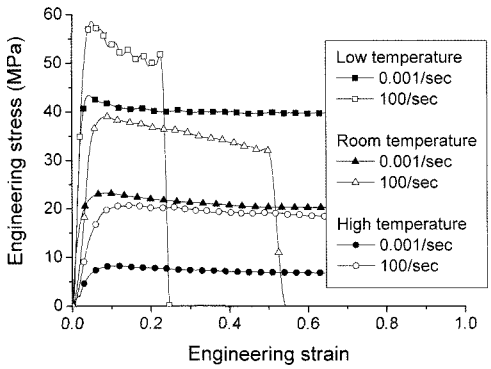

Figure 7. Engineering stress–strain curves of a polypropylene at the strain rate of 0.001/sec and 100/sec at the low, room and high temperatures.

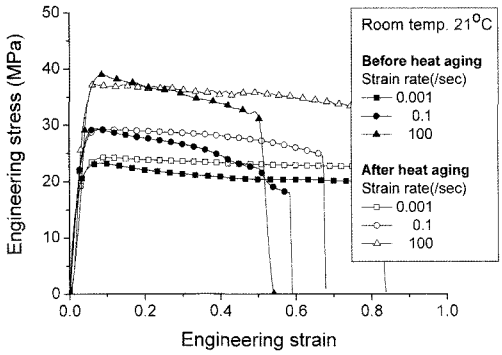

Figure 8. Engineering stress–strain curves at the room temperature (21°C) for a polypropylene before and after heat aging.

is about 90% higher than that at the room temperature and 440% higher than that at the high temperature. The fracture elongation at the high temperature is over 100% while the fracture elongation at the room temperature ranges from 50% to 70% and the fracture elongation at the low temperature ranges from 18% to 40% in dynamic tensile tests. At the low and room temperature, the fracture elongation has the minimum value at the strain rate of 0.1/sec while it has the minimum value at the strain rate of 100/sec at the high temperature.

The effect of the heat aging is also evaluated at the room temperature as shown in Figure 8. Heat aging was imposed in a way that the specimen was placed in the furnace at the temperature of 107°C for 240 hours and cooled down at the room temperature.

The strain rate sensitivity of the yield stress gives interesting results as shown in Figure 9. The strain rate sensitivity after heat aging increases at the low strain rate, but decreases at the mid-range of the strain rate, and then increases again at the high strain rate while the strain rate sensitivity before heat aging increases monotonically with respect to the strain rate. It is because the heat aging

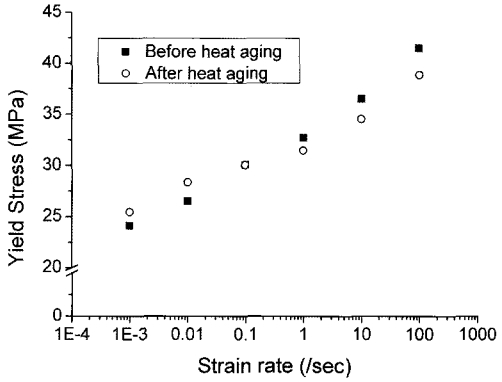

Figure 9. Strain rate sensitivity of a polypropylene at the room temperature (21°C) before and after heat aging.

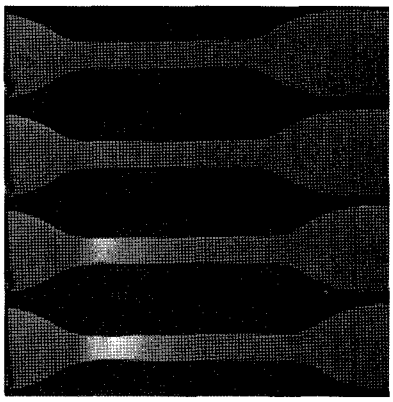

Figure 10. Deformed shapes of the ASTM IV specimen at the strain rate of 100/sec.

causes drop in the yield strength of a polypropylene at the high speed deformation while vice versa at the low speed deformation. However, the strain hardening increases after heat aging regardless of the strain rate as shown in Figure 8. The fracture elongation after heat aging is larger than that before heat aging.

2.4. Experimental Observation

Sequential deformed shapes of a real ASTM IV specimen are shown in Figure 10. Since the elongation tends to be localized after the onset of yield causing inhomogeneous deformation and the necking occurs at the small amount of total elongation, the conventional extensometry method is not applicable to measurement of elongation in the tensile test of polymer specimens. Figure 10 demonstrates that deformation is localized only in a small portion of the whole gauge length. The strain level at the necking region should be higher than that obtained by the conventional extensometry method in the average sense and the cross-sectional area at the necking region should be smaller than that obtained by the conventional extensometry method. In order to modify the stress–strain curve, the slope of the stress–strain curve needs to be corrected sequentially by the result of the finite element analysis with a new specimen using an optimization scheme. The new specimen is convenient for the finite element analysis since the necking always takes place at the center of the arc region.

Figure 11. Half model of the new specimen.

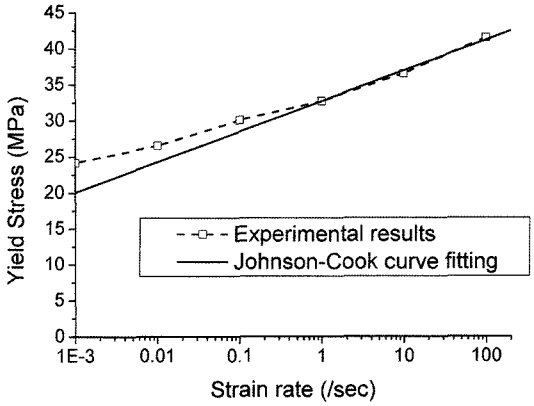

Figure 12. Johnson–Cook curve fitting of a polypropylene at the room temperature.

3. FINITE ELEMENT ANALYSIS

3.1. Analysis Conditions

A half model of the new specimen is shown in Figure 11. The finite element mesh system has 8004 brick elements with six layers through the thickness direction. One end of the specimen is pulled at the speed of 3.3 m/sec while the other end is fixed. Finite element simulation was carried out using LS-DYNA 3D. The Johnson–Cook model was adopted in calculation as shown in Figure 12 and Equation (1) in order to consider the strain rate hardening effect.

$$\sigma=(A+B\varepsilon_p^n)[1+C\ln(\dot{\varepsilon}/\dot{\varepsilon}_0)](1-T^{*m})$$

$$\text{where } T^*=\frac{T-T_{room}}{T_{melt}-T_{room}} \tag{1}$$

Since the slope of the flow stress is determined by a value of B, the value of B is modified in further analysis using an optimization scheme.

3.2. Analysis Results

Finite element analysis of a tensile test with the new specimen was carried out with the stress–strain curves

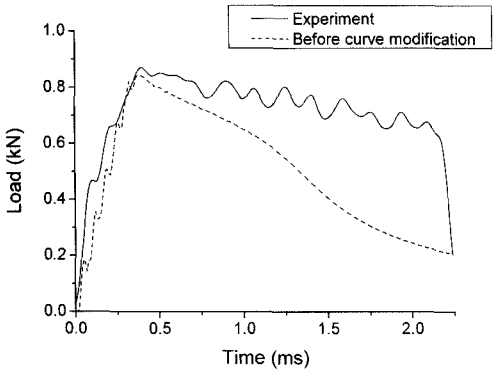

Figure 13. FEA result before the modification of the stress–strain curve compared to the experimental result.

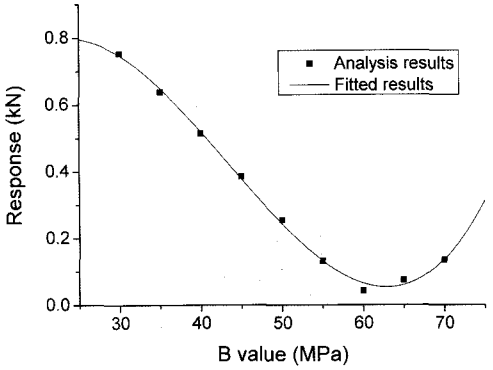

Figure 14. DOE results and fitted curve of wide range optimization.

obtained by the conventional extensometry method. Figure 13 shows the load–time curve obtained from the finite element analysis compared to the experimental result. The comparison shows large discrepancy between the experimental result and the analysis result after yielding. The discrepancy becomes larger as deformation proceeds. The reason is that the finite element analysis was carried out with the stress–strain curve obtained by the conventional extensometry method with the ASTM IV specimen undergoing inhomogeneous deformation. For the reason, the stress–strain curve needs to be modified for accurate mechanical properties in application to computer aided design and analysis. The slope of the stress–strain curve is modified based on experimental observations by changing a value of B in the Johnson–Cook model using an optimization scheme.

Optimization procedure is executed according to the formulation (2).

$$\text{Min. } R=\sqrt{\sum_{i=1}^{N}[f_i(B)-F_i]^2} \qquad (2)$$

s.t. $30 \le B \le 70$

where, f_i: Load obtained from finite element analysis at the i-th sampling point

F_i: Load obtained from experiment at the i-th sampling point

The objective function R is the least square value of the total sum of the discrepancies between the load obtained from the finite element analysis and the load from the experiment at seven sampling points of 0.6, 0.8, 1.0, 1.25, 1.5, 1.75 and 2.0 msec. The value of B is subjected to ranging from 30 to 70 MPa to search for the optimum point since the value of B is originally obtained as 31.06 MPa and it needs to be modified to a larger value. Nine runs for a design variable of B were performed and the results in each run are tabulated in Table 1. The response is interpolated by the third order polynomials as shown in Equation (3) and plotted in Figure 14.

$$R=-0.5166+0.1232\times B-0.00350\times B^2+0.00002607\times B^3 \qquad (3)$$

According to the result of nine runs, the optimum point is known to locate at a point near 60 MPa. The second DOE was carried out with finer interval of the value of B. In the range of B from 59 to 63 MPa, nine analyses were

Table 1. DOE table for wide range optimization.

Number of run	B (MPa)	R (kN)
1	30	0.7306
2	35	0.6377
3	40	0.5143
4	45	0.3859
5	50	0.2548
6	55	0.1309
7	60	0.0434
8	65	0.0745
9	70	0.1343

Table 2. DOE table for local range optimization.

Number of run	B (MPa)	R (kN)
1	59	0.0554
2	59.5	0.0493
3	60	0.0434
4	60.5	0.0397
5	61	0.0381
6	61.5	0.0395
7	62	0.0416
8	62.5	0.0456
9	63	0.0515

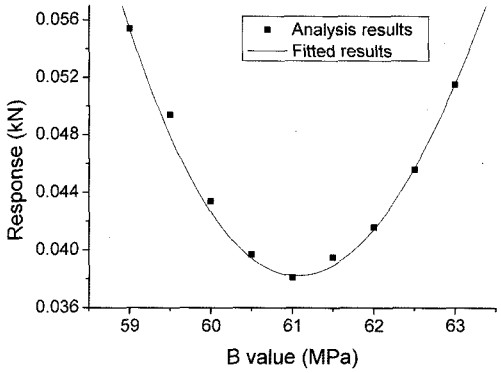

Figure 15. DOE results and fitted curve of local range optimization.

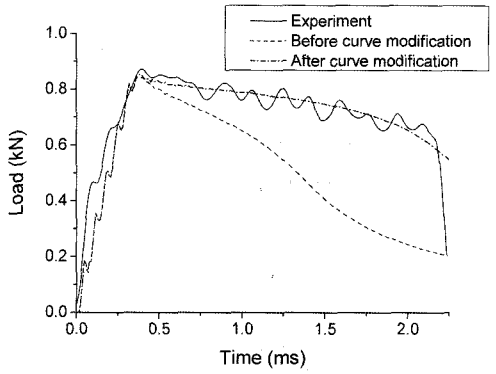

Figure 16. Experimental load–time curve and the load–time curve from the finite element analysis before and after the modification of the stress–strain curve.

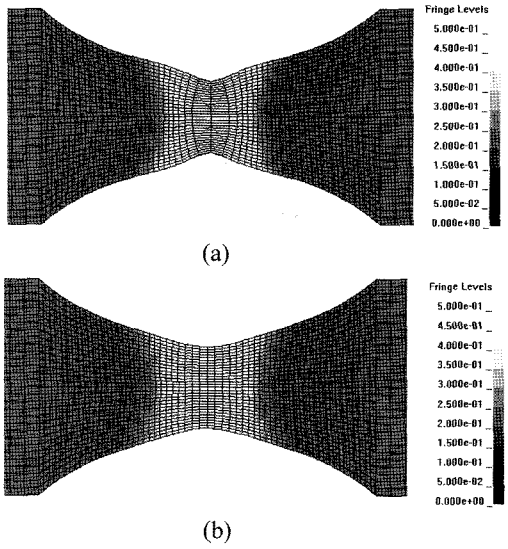

Figure 17. Deformed shapes and contours of the effective plastic strain at the elapsed time of 1.5 msec: (a) before stress–strain curve modification; (b) after stress–strain curve modification.

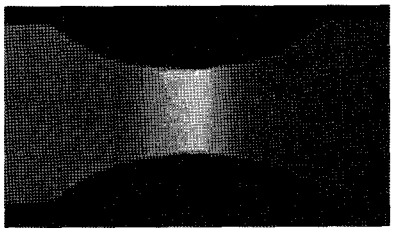

Figure 18. Deformed shape of the new specimen at the pulling speed of 3.3 m/sec.

performed as the DOE table in Table 2. The response is interpolated by the third order polynomials as shown in Equation (4) and plotted in Figure 15.

$$R=-41.9076-1.825\times B-0.02612\times B^2+0.0001219\times B^3 \quad (4)$$

The optimum value of R is obtained at the point where the value of B is 61.03 MPa. The load–time curve obtained from the finite element simulation with the optimum value of B is shown in Figure 16 which shows that the simulation result coincides with the experimental result. Figure 17 (a) shows that the middle of the arc region forms a sharp edge unlike the deformed shape in the experiment while Figure 17 (b) shows that the middle of the arc region remains round after the modification of the stress–strain curve, which is similar to the deformed shape in the experiment as shown in Figure 18. It is noted that the concentration of deformation at the middle of the arc region is relaxed with a larger value of B obtained from the optimization and the specimen sustains the tensile load effectively in a wider region.

4. CONCLUSION

The tensile characteristics of a polypropylene used in an instrument panel of a car were evaluated at the low temperature (−30°C), the room temperature (21°C), and the high temperature (85°C) with the variation of the strain rate. The effect of heat aging on the material properties was also investigated by the experiment.

The experimental result shows that the flow stress decreases remarkably, but the fracture elongation and the strain rate sensitivity of a polypropylene increases as the temperature increases. The fluctuation of the flow stress was observed with respect to the strain rate at the low temperature. The result shows that the heat aging enhances the strain hardening and fracture elongation.

This paper proposes a useful method to obtain the true stress–strain curve by modification of the experimental stress–strain curve with the help of finite element analysis for optimization of the material constant. The result demonstrates that simulation result with the true stress–strain curve modified is closely coincident with the experimental result while there is large discrepancy

between the experimental result and the simulation result with the stress–strain curve before modification.

REFERENCES

Arruda, E. M., Boyce, M. C. and Jayachandran, R. (1995). Effects of strain rate, temperature and thermomechanical coupling on the finite strain deformation of glassy polymers. *Mechanics of Materials*, **19**, 193–212.

Brooks, N. W. J. and Mukhtar, M. (2000). Temperature and stem length dependence of the yield stress of polyethylene. *Polymer*, **41**, 1475–1480.

Cook, W. D., Mayr, A. E. and Edward, G. H. (1998) Yielding behavior in model epoxy thermosets-I. Effect of strain rate and composition. *Polymer* **39**, **16**, 3719–3724.

G'Sell, C., Hiver, J. M. and Dahoun, A. (2002). Experimental characterization of deformation damage in solid polymers under tension, and its interrelation with necking. *Int. J. Solids and Structures*, **39**, **13–14**, 3857–3872.

Huh, H., Lim, J. H., Song, J. H., Lee, K. S, Lee, Y. W., and Han, S. S. (2003). Crashworthiness assessment of side impact of an auto-body with 60TRIP steel for side members. *Int. J. Automotive Technology* **4**, **3**, 149–156.

Kang, W. J. and Huh, H. (2000). Crash analysis of auto-body structures considering the strain-rate hardening effect. *Int. J. Automotive Technology* **1**, **1**, 35–41.

Kim, K. J. (2006). Serration mechanism of AA5182/Polypropylene/AA5182 sandwich sheets. *Int. J. Automotive Technology* **7**, **4**, 485–492.

Lim, J. H., Kim, S. B., Kim, J. S., Huh, H., Lim, J. D. and Park, S. H. (2005). High speed tensile tests of steel sheets for an auto-body at the intermediate strain rate. *Trans. Korean Society Automotive Engineers* **13**, **2**, 127–134.

Machida, T. and Lee, D. (1998). Deep drawing of polypropylene sheets under differential heating conditions. *Polymer Eng. Sci.*, **28**, 405–412.

Marquez-Lucero, A., G'Sell, C. and Neale, K. W. (1989). Experimental investigation of neck propagation in polymers. *Polymer*, **30**, 636–642.

Mayr, A. E., Cook, W. D. and Edward, G. H. (1998). Yielding behavior in model epoxy thermosets-II. Temperature dependence. *Polymer* **39**, **16**, 3725–3733.

Parsons, E. M., Boyce, M. C., Parks, D. M. and Weinberg, M. (2005). Three-dimensional large-strain tensile deformation of neat and calcium carbonate-filled high-density polyethylene. *Polymer*, **46**, 2257–2265.

The Korea Society of Automotive Engineers (1996). *Technical Handbook of Automobile*. Seoul. Korea.

Walley, S. M., Field, J. E., Pope, P. H. and Stafford, N. A. (1989). A study of the rapid deformation behavior of a range of polymers. *Philos. Trans. Soc. London* **A**, **328**, 783–811.